Available online at www.sciencedirect.com
SCIENCE DIRECT®
ELSEVIER
The International Journal of Biochemistry & Cell Biology 37 (2005) 590–603
IJBCB
www.elsevier.com/locate/biocel

ADAM15 decreases integrin αvβ3/vitronectin-mediated ovarian cancer cell adhesion and motility in an RGD-dependent fashion

Veronika Beck[a,1], Hannes Herold[a,1], Anke Benge[a], Birgit Luber[b], Peter Hutzler[c], Harald Tschesche[d], Horst Kessler[e], Manfred Schmitt[a], Harald-Gerhard Geppert[d], Ute Reuning[a,*]

[a] *Clinical Research Unit, Department of Obstetrics and Gynecology, Technische Universität München (TUM), D-81675 Munich, Germany*
[b] *Institute of Pathology, Technische Universität München (TUM), D-81675 Munich, Germany*
[c] *Institute of Pathology, GSF Research Center, D-85758 Neuherberg, Germany*
[d] *Department of Chemistry, Biochemistry I, University of Bielefeld, D-33615 Bielefeld, Germany*
[e] *Institute of Organic Chemistry and Biochemistry, TUM, Lichtenbergstr. 4, D-85747 Garching, Germany*

Received 6 January 2004; received in revised form 5 August 2004; accepted 16 August 2004

Abstract

We have recently described that integrin αvβ3 upon interaction with its major extracellular matrix ligand vitronectin induces adhesion, motility, and proliferation of human ovarian cancer cells. Due to the important function of αvβ3 in cancer cell biology, it has been the effort of many scientific approaches to specifically target αvβ3-mediated cell adhesion and tumorbiological effects arising thereof by synthetic integrin antagonists. More recently, proteins of the ADAM family have been recognized as naturally occurring integrin ligands. Among those, human ADAM15 which encompasses the integrin binding RGD motif was shown to interact with integrin αvβ3. Thus, we investigated in human ovarian OV-MZ-6 cancer cells, expressing both ADAM15 and αvβ3, whether ADAM15 might affect αvβ3-mediated tumorbiological effects. We stably (over)expressed ADAM15 or its extracellular domain in OV-MZ-6 cells as well as respective ADAM15 mutants containing the tripeptide SGA instead of RGD. Cells (over)expressing ADAM15-RGD exhibited a significantly reduced αvβ3-mediated adhesion to vitronectin. Also, a significant time-dependent decline in numbers of cells cultivated on vitronectin was noticed. This effect was found to be rather due to impaired αvβ3-mediated cell adhesion than decreased cell proliferation rates, since de novo DNA synthesis was not significantly altered by elevated ADAM15 expression. Moreover, a substantially decreased random cellular motility was noticed as a function of ADAM15 encompassing an intact RGD motif. In conclusion, our results point to a physiological role

* Corresponding author. Tel.: +49 89 4140 7407; fax: +49 89 4140 7410.
E-mail address: ute.reuning@lrz.tum.de (U. Reuning).
[1] Both authors contributed equally.

1357-2725/$ – see front matter
doi:10.1016/j.biocel.2004.08.005

of ADAM15 as a natural binding partner of integrin αvβ3 thereby loosening tumor cell adhesion to the underlying matrix and regulating tumor cell migration and invasion.

Keywords: ADAM15; Ovarian cancer; Integrin αvβ3; Cell adhesion; Cell motility

1. Introduction

ADAM proteins constitute a family of more than 30 transmembrane as well as secreted glycoproteins which are ubiquitously distributed in human and animal tissues, such as brain, testis, ovary, breast, and muscle. Most interestingly, a high sequence similarity of ADAMs to snake venom disintegrins and metalloproteases has been described (Weskamp & Blobel, 1994; Wolfsberg, Primakoff, Myles, & White, 1995; Wolfsberg & White, 1996). ADAM functions include proteolysis, cell adhesion, cell fusion, protein ecto-domain shedding, and intracellular signaling (Bridges, Hanson, Tani, Mather, & Bowditch, 2003; Herren, 2002; Primakoff & Myles, 2000). All ADAMs are composed of distinct molecular domains, comprising a pro-domain, a metalloproteinase, and a disintegrin domain, plus a cysteine-rich region containing an epidermal growth factor (EGF) repeat, a transmembrane domain, and a cytoplasmic tail. Although all ADAMs share a rather stably conserved metalloprotease domain, only a subset of ADAM family members has been shown to be catalytically active. By this property, some ADAMs are involved in shedding of biologically important cell surface proteins such as tumor necrosis factor-α (ADAM17 or TACE) (Blobel, 1997; Kheradmand & Werb, 2002), Alzheimer amyloid precursor protein (ADAM10 and 17) (Buxbaum et al., 1998; Lammich et al., 1996), and the Notch ligand delta1 (ADAM10) (Blobel, 1997; Pan & Rubin, 1997; Qi et al., 1999; Six et al., 2003). The disintegrin domains of ADAMs represent (potential) binding sites for cell adhesion- and signaling-receptors of the integrin superfamily. The integrin binding motif is represented by a characteristic tripeptide sequence which is exposed within a loop and determines together with the N- and C-terminal flanking regions the specificity and affinity of ADAMs towards distinct integrins (Nath et al., 2000; Wolfsberg & White, 1996; Zhou, Graham, Russell, & Croucher, 2001). Integrins recognize such tripeptide motifs also within ECM proteins thereby mediating cell adhesion to an underlying growth substrate. Via their cytoplasmic regions which interact with cytoskeletal proteins, integrins provide a physical connection between the internal and external cellular environment and constitute an interface in which mechanical forces, cytoskeletal reorganization, and biochemical signals may convene. Furthermore, by triggering the assembly of signaling molecules, integrins take over key functions during intracellular signal transduction across the plasma membrane (Damsky & Werb, 1992; Giancotti & Ruoslahti, 1999; Hynes & Lander, 1992; Ruoslahti & Reed, 1994; Schwartz & Ginsberg, 2001). Upon competition with ECM proteins for integrin binding, ADAMs are thought to be involved in the regulation of cell/ECM- and cell/cell-interactions in many (patho-) physiological settings.

Human ADAM15 is unique among ADAM proteins since it contains the integrin binding motif Arg-Gly-Asp (RGD) within its disintegrin region (Bosse et al., 2000; Krätzschmar, Lum, & Blobel, 1996; Lum, Reid, & Blobel, 1998; Nath et al., 1999). Integrin binding capacity of ADAM15 has been observed, e.g. for integrins αvβ3 and α5β1 (Nath et al., 1999, 2000; Zhang, Kamata, Yokoyama, Puzon-McLaughlin, & Takada, 1998; Zhou et al., 2001), as well as α9β1 (Eto et al., 2000) in studies employing ADAM15-derived peptides, recombinant, soluble ADAM15 proteins, or hybrid molecules containing fragments of the ADAM15 molecule, immobilized onto solid supports. Moreover, ADAM15 is 1 of 17 ADAMs containing a consensus sequence predicted to be the catalytic site of an active zinc-dependent metalloprotease. Still, the natural substrate of ADAM15 remains to be identified (Lum et al., 1998). Expression levels of ADAM15 have been found to be elevated in numerous tissues undergoing extensive remodeling. As such, ADAM15 is upregulated in atherosclerotic lesions when compared to normal vessels coinciding with elevated integrin αvβ3 expression in endothelial cells (Herren, Raines, & Ross, 1997). Also, a strong increase of ADAM15 protein

and mRNA levels was noticed in rheumatoid tissue and chondrosarcoma, indicating an involvement in cartilage remodeling (Böhm, Aigner, Blobel, Kalden & Burkhardt, 2001). Moreover, ADAM15 mRNA levels are increased in atrial fibrillation and dilatation, pointing to a role in cardiac tissue remodeling (Arndt et al., 2002). Since, it has been proposed that ADAM15 may play a role in malignancy, it was determined whether the ADAM15 gene is located in a known disease susceptibility region. Indeed, the ADAM15 gene was localized to human chromosome band 1q21.3 that is amplified in several types of cancers (Kärkkäinen, Karhu, & Huovila, 2000; Wu, Croucher, & McKie, 1997).

In earlier studies, we demonstrated that the human ovarian cancer cell line OV-MZ-6 in an αvβ3-dependent fashion binds to the ECM protein vitro nectin (VN), which is one of the abundant adhesion substrata in normal ovarian epithelium as well as in differentiated ovarian tumors (Carreiras, Cruet, Staedel, Sichel, & Gauduchon, 1999; Hapke et al., 2001). During ovarian cancer metastasis, tumor cells spread within the peritoneal cavity, adhere to local organs in an integrin-mediated fashion and start proliferation. Besides the implication of αvβ3 in tumor angiogenesis (Brooks et al., 1994), several lines of evidence point to its role during ovarian cancer cell invasion, and the generation of growth and survival signals during tumor metastasis (Cruet, Salamanca, Mitchell, & Auersperg, 1999; Van der Flier & Sonnenberg, 2001).

Despite the knowledge that both the disintegrin and the metalloprotease domain of ADAM15 are potentially capable of modulating integrin-mediated cell adhesive events, their precise functions are still uncertain in most cases. Thus, in the present study, we established ADAM15 expressing experimental human ovarian cancer cell models in order to investigate the involvement of ADAM15 in the regulation of cancer cell adhesion, migration, and proliferation.

2. Materials and methods

2.1. Materials

Cell culture media (Dulbecco's Modified Eagle Medium, DMEM), phosphate-buffered saline (PBS), media supplements, Lipofectin®, and VN were obtained from Gibco/Becton Dickinson, Eggenstein, Germany. Microchamber slides were purchased from Nunc Lab-Tek, Naperville, IL, USA. [^{3}H]-methyl thymidine was from ICN, Eschwege, Germany. Monoclonal antibodies (mAb) directed to c-myc as well as the eukaryotic expression vector pcDNA3.1/Myc-His were purchased from Invitrogen, Karlsruhe, Germany. The rabbit pAb directed to ADAM15 was kindly supplied by Prof. Carl Blobel, Memorial Sloan Kettering Cancer Center, New York, NY, USA. Fluoroisothiocyanate (FITC)-labeled mAb directed to αvβ3 (clone LM609) was ordered from Chemicon, Hofheim, Germany. Polyclonal goat antibodies directed to actin were purchased from Santa Cruz Biotechnology Inc., Santa Cruz, CA, USA. The ECL Western blot detection system was purchased from Amersham Biosciences (Freiburg, Germany). Nitrocellulose was obtained by Schleicher & Schüll, Dassel, Germany. Collagen type I (Col-I) and type IV (Col-IV), the hexosaminidase reagent *p*-nitrophenyl-*N*-acetyl-beta-D-glucosaminide, MTT (3-(4,5-dimethylthiazol-2-yl)-2,5-diphenyl tetrazolium bromide thiazolyl blue), bovine serum albumin (BSA), and paraformaldehyde (PFA), were from Sigma, Deisenhofen, Germany. Alexa-488-labeled goat-anti-mouse IgG and goat-anti-rabbit IgG were purchased from Molecular Probes, Eugene, OR, USA. The RNA isolation kit "RNA-Clean" was ordered from TM System, AGS, Heidelberg, Germany. DNase I and reverse transcriptase (RT) were obtained from Roche Diagnostics, Penzberg, Germany. The mutagenesis kit Transformer™ site-directed mutagenesis was purchased from Clontech, Palo Alto, CA, USA. Oligodeoxynucleotides were synthesized at Metabion, Martinsried, Germany. Protein concentrations were determined using the BCA protein reagent kit from Pierce, Rockford, IL, USA.

2.2. Cell culture

Origin and cultivation of the human ovarian cancer cell line OV-MZ-6 has been described previously (Möbus et al., 1992; Reuning et al., 1995). Generation of stably transfected OV-MZ-6 cell clones, exhibiting up to 10-fold elevated expression levels of αvβ3 was described earlier (Hapke et al., 2001). As an alternative and heterologous cellular ADAM15 expression system we also transfected Chinese hamster ovary

cells (CHO) which were cultivated and transfected according to the procedures described for OV-MZ-6 cells.

2.3. ADAM15 cDNA cloning and in vitro mutagenesis

Human ADAM15 was cloned by reverse transcriptase polymerase chain reaction (RT-PCR) from the human ovarian cancer cell line OV-MZ-6. After reverse transcription of total RNA, the following primer pairs were used for PCR: ADAM15-full length (FL): ADAM15-5′: 5′-AAA AAA AGC TTA TGC GGC TGG CGC TGC TC-3′ and ADAM15-3′: 5′-AAA CAT CTA GAG AGG TAG AGC GAG GAC AC-3′. For cloning of cDNAs solely encoding the extracellular domain of human ADAM15 (ADAM15-ecto), we employed the primers: Ecto-5′: 5′-AAA AAA AGC TTA TGC GGC TGG CGC TGC TC-3′ and Ecto-3′: 5′-AAA AAT CTA GAG CTG GTT GCT TTG AGC TGA-3′. In addition, ADAM15 mutants were generated in which within the disintegrin domain, Arg^{484} was changed to Ser and Asp^{486} to Ala, resulting in the non-integrin binding motif SGA. For in vitro site-directed mutagenesis, we used the primer: 5′-GTG TCG TCC TAC CAG TGG GGC TTG TGA CTT GCC TG-3′ and the kit Transformer^{TM} (Clontech) according to the manufacturers' recommendations. The PCR products were directionally subcloned into the polylinker sites *Hin*dIII and *Bam*HI of the expression vector pcDNA3.1/Myc-His. All constructs were identified by restriction mapping and verified by DNA sequencing.

2.4. Cell transfections and stable (over)expression of ADAM15 and its variants

Transfection of OV-MZ-6 cells with the different ADAM15 cDNA variants and isolation of transfected OV-MZ-6 cell clones were conducted upon neomycin selection as described earlier (Hapke et al., 2001). Several OV-MZ-6 cell clones isolated from each transfection category were tested for ADAM15 expression by immunostaining and subsequent evaluation by confocal laser scanning microscopy (CLSM). For the generation of the respective human ADAM15 expressing CHO cell clones, the same procedures were performed as outlined for OV-MZ-6 cells.

2.5. Immunostaining and confocal laser scanning microscopy (CLSM)

Detection of ADAM15: ADAM15-transfected OV-MZ-6 cell clones were cultivated overnight in microchamber slides. Cells were then washed in PBS, fixed in 2% (w/v) PFA (20 min, room temperature) and a mAb directed to the c-myc epitope contained within the generated ADAM15 fusion proteins (1 μg/ml) added for 2 h at room temperature. After repeated washes in PBS, an Alexa-488-conjugated goat-anti-mouse IgG (50 ng/ml) was added in PBS/1% (w/v) BSA for 45 min at room temperature. As an additional proof of ADAM15 expression, immunostaining procedures were performed using an antiserum containing pAb directed to the extracellular domain of human ADAM15 at a dilution of 1:100 using an Alexa-488-conjugated goat–anti-rabbit IgG as secondary antibody. Double immunostaining of ADAM15 and αvβ3: In order to study cell surface distribution of ADAM15 and αvβ3 in human OV-MZ-6 cells, immunostaining procedures were conducted in the presence of both a pAb directed to the extracellular domain of ADAM15 and a FITC-labeled mAb directed to αvβ3. For detection of binding of the ADAM15-pAb, an Alexa-568-labeled goat-anti-rabbit IgG was used. Fluorescence signal intensity was visualized by CLSM using the Zeiss Axiovert 35 microscope (Göttingen, Germany) at 488 and 568 nm, respectively. Staining procedures in the presence of the secondary Ab alone or using an irrelevant control IgG as the primary Ab served as controls. In order to visualize the fluorescence staining intensity, for scanning, the look-up table glowOv/Un LUT provided with the CLSM scanning software (Leica, Heidelberg, Germany) was applied. This look-up table converts the staining intensities into the colors of a pseudo glow scale: low intensity (red), medium intensity (yellow), and high intensity (white).

2.6. Semi-quantitative RT-PCR analysis of ADAM15 mRNA expression

RT-PCR analyses for the determination of ADAM15 mRNA concentrations in OV-MZ-6 cells were performed as described earlier (Hapke et al., 2001; Reuning et al., 1999) by applying the following ADAM15 primers: 5′-GGC TGG CAG TGT CGT CCT ACC AGA GGG G-3′ and 5′-GGT GCA

CCC AGC TGC AGT TCA GCT CAG TCC-3′ (amplicon size: 420 bp). Equal RNA concentrations and efficiency of RT reactions were controlled by simultaneous amplification of the house keeping gene glyceraldehyde 3-phosphate dehydrogenase (GAPDH) within the same PCR reaction (amplicon size: 194 bp) using the primers: GAPDH-5′: 5′-CCA TGG AGA AGG CTG GGG-3′ and GAPDH-3′: 5′-CAA AGT TGT CAT GGA TGA CC-3′. ADAM15 and GAPDH amplification products were electrophoresed on Tris–borate–EDTA–polyacrylamide gels. Signal intensity was evaluated by densitometrical scan using the Scion Image Software (Scion Corporation, Frederick, MD, USA). Data are given as the ratio of ADAM15 to GAPDH amplification products.

2.7. Western blot analysis

Detection of ADAM15 protein in transfected cell clones: Cell lysates were prepared in RIPA buffer and protein concentrations determined as previously described (Hapke et al., 2001). Proteins were separated on 12% (w/v) sodium dodecyl sulphate (SDS)–polyacrylamide gels and transferred to nitrocellulose membranes. After blocking the membranes in PBS, 3% (w/v) BSA, 0.05% (v/v) Tween-20, overnight at 4 °C, the polyclonal rabbit antibody directed to the cytoplasmic domain of human ADAM15 (2 μg/ml) was added in PBS, 0.05% (v/v) Tween-20, 1% (w/v) BSA overnight at 4 °C. After repeated washes in PBS, the secondary horseradish peroxidase-conjugated goat-anti-rabbit antibody (1:8000) was added for 90 min at room temperature. Reactive proteins were visualized by the ECL Western blot detection system according to the manufacturers' recommendations. In order to normalize for equal protein loading in each lane, a second abundant protein, actin, was detected on the identical membranes. For this, the nitrocellulose membranes were stripped in 200 mM glycine, pH 2.2, 0.1% (w/v) SDS, 1% (v/v) Tween-20, for 60 min at room temperature, followed by three washes in PBS. After blocking the membranes again in PBS, 3% (w/v) BSA, 0.05% (v/v) Tween-20 overnight at 4 °C, they were incubated overnight at 4 °C with a polyclonal goat antibody directed to actin at a final concentration of 0.25 μg/ml. After repeated washes in PBS, as secondary antibody, a horseradish peroxidase-conjugated polyclonal rabbit-anti-goat IgG (0.1 μg/ml) was added for 2 h at room temperature. Reactive proteins were visualized by ECL. Evaluation of signal intensity by Western blot analyses was performed by densitometrical scanning using the Scion Image Software. Data are given as ratio of signal intensity for ADAM15 versus those for actin.

2.8. In vitro cell/ECM adhesion assay

Cell adhesive capacity to different purified ECM proteins was assessed by means of a chromogenic assay as described earlier (Hapke et al., 2001; Landegren, 1984). Significance of differences in data were determined by one-tailed non-parametric Mann–Whitney tests.

2.9. Cell proliferation assays

Cell counting: Cells were seeded into 24-well cell culture plates precoated with different purified ECM proteins and after distinct time intervals, cell numbers counted upon trypan blue exclusion using a Neubauer hemocytometer. MTT-assay: Cells were seeded at a density of 5×10^3 cells per 96-well onto ECM- or non-coated cell culture plates. After distinct time intervals, MTT (200 μg/ml) was added and incubated with cells for another 2 h at 37 °C. The medium was aspirated and 100 μl of DMSO added followed by colorimetrical measurements at 590 nm (Carmichael, DeGraff, Gazdar, Minna, & Mitchell, 1987). Incorporation of [^{3}H]-methyl thymidine: 96-well cell culture dishes were precoated with different purified ECM proteins. After blocking the cell growth areas in PBS, 2% (w/v) BSA and subsequent washes in PBS, 2×10^4 OV-MZ-6 cells were seeded in each well and cultivated for up to 4 days. Then, [^{3}H]-methyl thymidine (25 μCi/ml) was added for another 6 h. Cell lysates were harvested using the Harvester 96 (TomTec, Orange, CN) by transferring them onto a glassfiber filter (Printed Filtermat A, Wallac, Turku, Finland). Thereafter, wax (Melti Lex, Wallac, Turku, Finland) was melted over the filters and the amount of [^{3}H]-methyl thymidine, incorporated into cellular DNA, determined by scintillation counting. Radioactivity incorporated into cellular DNA, expressed as cpm values, was normalized to the protein concentrations of each cell sample as a measure of cell numbers as previously described (Hapke et al., 2003).

2.10. Cell motility assays by time lapse confocal laser scanning microscopy

Specialized cell culture glas bottom dishes (P45G-0-14-C-gm; MatTek Corporation, Ashland, USA) were coated for 2 h at 37 °C with purified ECM proteins (10 μg/ml) (Hapke et al., 2001), blocked in PBS/2% (w/v) BSA for 2 h, and thereafter washed in PBS. 1.5×10^5 OV-MZ-6 cells/dish were seeded in 5 ml of DMEM, 10% (v/v) FCS. After cell adhesion for 50 min, cells were examined on a LSM 510 (Zeiss, Jena, Germany) with an inverted stand Axiovert 100 M including an incubation system with temperature and CO_2 control (PeCon GmbH, Erlbach, Germany). Phase contrast images were taken using a lens PlanNeofluar 20×/0.5 PH2 every other 3 min within 8 h at 543 nm and stored using the software LSM 510 (Zeiss). Lengths of cellular tracks over time were determined based on the movement of the center of the nuclei using the Zeiss Software AIM 3.0 (Zeiss).

3. Results

3.1. Expression of ADAM15 and variants thereof in human ovarian OV-MZ-6 cancer cells

We generated and isolated OV-MZ-6 cell clones stably transfected with cDNAs encoding wild-type (WT) full length ADAM15 containing the integrin binding motif RGD (FL-RGD) and an ADAM15 mutant in which the RGD motif has been substituted by the tripeptide motif SGA (FL-SGA). There are reports that several transmembrane members of the ADAM family are shed from cell surfaces thereby releasing the extracellular domain as a diffusable potential integrin antagonist (Herren et al., 1997). Based on this, we designed, in addition, two ADAM15 cDNA constructs encompassing solely the extracellular domain lacking the transmembrane and cytoplasmic region (Ecto-RGD). Also hereby, the truncated ADAM15 mutant encompassing a SGA (Ecto-SGA) served as a control. The extent of ADAM15 antigen expression was determined by immunostaining and subsequent evaluation of ADAM15 expression levels by CLSM. In one immunostaining approach, we utilized a mAb directed to the c-myc epitope contained within the ADAM15/c-myc fusion proteins (Fig. 1A). OV-MZ-6 cell clones stably transfected with either of the four different ADAM15 cDNA constructs (FL-RGD, FL-SGA, Ecto-RGD, or Ecto-SGA) resulted in significantly elevated fluorescence signal intensity indicating increased expression of the different ADAM15/c-myc fusion proteins when compared to OV-MZ-6 wild-type cells. By comparing the cell morphology of different ADAM15-transfected OV-MZ-6 cell clones it was obvious that the clones overexpressing ADAM15-RGD were less spread and displayed a more rounded morphology than wild-type, vector-, FL-SGA or Ecto-SGA-transfected cells. In a complementary immunostaining procedure, a specific pAb directed to the extracellular portion of ADAM15 was used confirming overexpression of ADAM15 FL-RGD over wild-type levels (Fig. 1B). In addition to ADAM15 detection at the protein level, we conducted semi-quantitative RT-PCR analyses in order to determine ADAM15 transcript concentrations. Fig. 1C depicts representative OV-MZ-6 cell clones of each transfection category exhibiting a comparable elevation of ADAM15 proteins (FL-RGD: 4.3-fold; FL-SGA: 4.6-fold; Ecto-RGD: 3.7-fold; Ecto-SGA: 3.1-fold) when compared to wild-type or vector-transfected cells. In addition, Western blot analyses using an antibody directed to the cytoplasmic domain of human ADAM15 were performed in order to detect ADAM15 protein expression in transfected cells. Densitometrical analysis and normalization to actin revealed that the independently isolated OV-MZ-6 cell clones used in the present study displayed comparable, up to four-fold elevated ADAM15 protein expression levels over vector-transfected control cells (Fig. 1D).

3.2. ADAM15 and integrin αvβ3 show similar distribution patterns on the OV-MZ-6 cell surface

Previously, we have shown that cultured human ovarian OV-MZ-6 cancer cells express integrin αvβ3 (Hapke et al., 2001), one of the reported integrin ligands for ADAM15 (Nath et al., 1999). Since human OV-MZ-6 cells also express ADAM15, we studied whether both proteins are expressed in close proximity on the OV-MZ-6 cell surface. Double immunostaining revealed a very similar distribution pattern of ADAM15 and αvβ3, respectively, suggesting that the two interaction partners may reside within close neighbourhood on the OV-MZ-6 cell surface (Fig. 2).

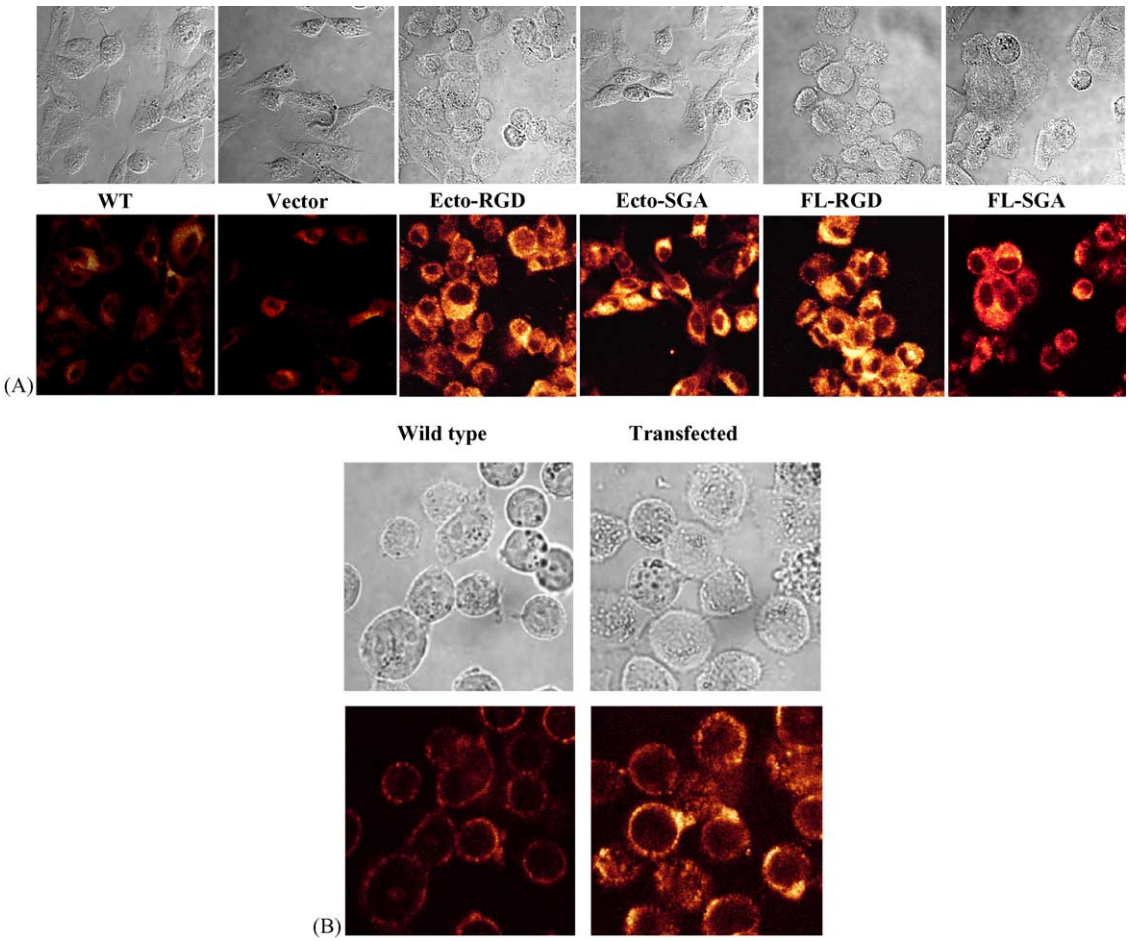

Fig. 1. Generation of OV-MZ-6 cells (over)expressing ADAM15 and variants thereof Immunocytochemistry and CLSM. OV-MZ-6 cells were grown on microchamber slides and immunostaining was performed as described under Section 2. (A) Immunostaining of ADAM15 with a c-myc mAb. One representative clone of each ADAM15 transfection category is depicted in comparison to wild-type (WT) and vector-transfected OV-MZ-6 cells. (B) Immunostaining of ADAM15 with a pAb directed to ADAM15. One representative OV-MZ-6 cell clone overexpressing ADAM15 FL-RGD is shown in comparison to ADAM15 wild-type expression. Transmission images (upper row) and respective fluorescence images (lower row) are depicted. (C) Semi-quantitative RT-PCR analysis of ADAM15 mRNA concentrations after OV-MZ-6 cell transfections with ADAM15 cDNAs. Total RNA of wild-type, vector- or ADAM15-transfected OV-MZ-6 cells were harvested, and RT-PCR analyses conducted as described. ADAM15 amplification products were electrophoresed on Tris–borate–EDTA–polyacrylamide gels. As controls served GAPDH PCR reactions. A representative experiment is depicted. Signal intensity was evaluated by densitometrical scanning using the Scion Image Software. Data are given as mRNA ratio between the signal intensity obtained for ADAM15 and GAPDH PCR products. (D) Western blot analysis of ADAM15 protein expression in transfected OV-MZ-6 cell clones. Western blot analysis was performed as described under Section 2. Membranes were first incubated with a polyclonal antibody directed to ADAM15, and then, after membrane stripping an antibody directed to actin added, in order to control for equal protein loading per lane. A representative Western blot is depicted together with the evaluation of signal intensity by densitometrical scanning. Data are given as ratio between intensity for ADAM15 vs. actin signals (M: marker; 1: vector; 2: FL-RGD #1; 3: FL-RGD #2; 4: FL-SGA #1; 5: FL-SGA #2).

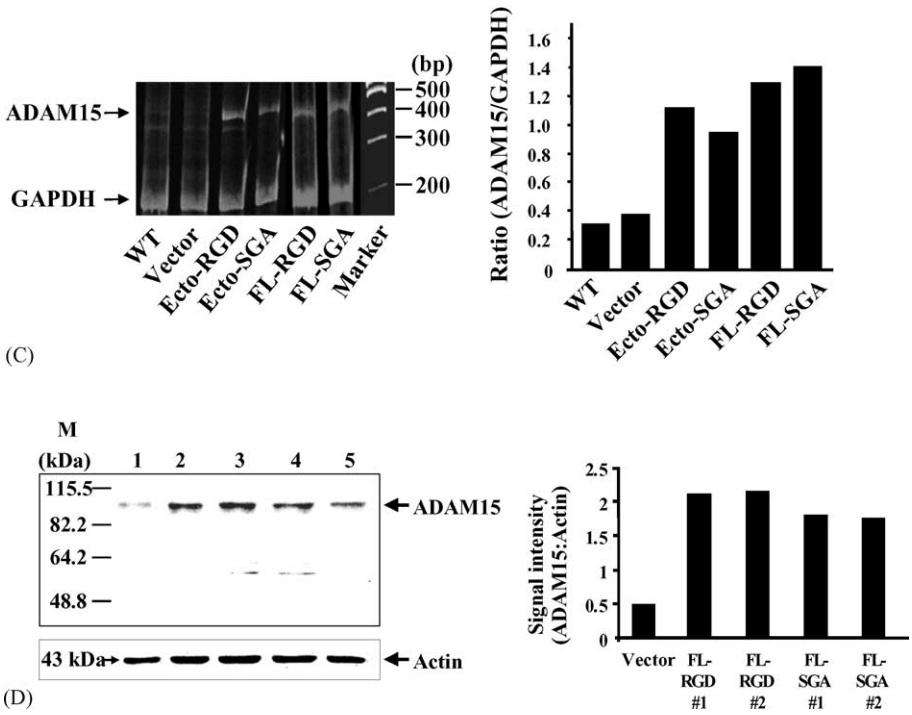

Fig. 1. (*Continued*).

3.3. Expression of human ADAM15 proteins encompassing an RGD motif significantly reduced integrin αvβ3-mediated OV-MZ-6 cell adhesion to vitronectin

In previous studies, we established ECM-dependent adhesion profiles for the human ovarian cancer cell line OV-MZ-6. Hereby we demonstrated that both the ECM protein VN as well as Col-IV provoke increased OV-MZ-6 cell adhesion, whereas cellular attachment to Col-I is significantly weaker and almost comparable to the cellular adhesive capacity observed on non-pretreated cell culture dishes (Hapke et al., 2001). Proof for an αvβ3-dependent cell contact to VN was obtained from competition studies with the synthetic αvβ3-directed cyclic peptide cRGDfV which inhibited

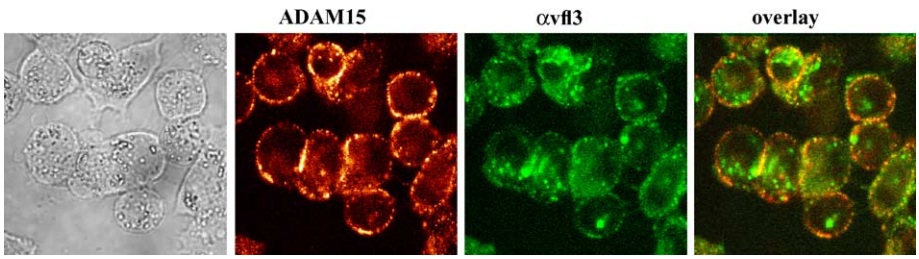

Fig. 2. Distribution patterns of ADAM15 and integrin αvβ3 on the surface of human OV-MZ-6 cells. Double immunostaining procedures were conducted in the presence of both, a pAb directed to the extracellular domain of ADAM15 and a FITC-labeled mAb directed to αvβ3. For detection of ADAM15, as secondary Ab, an Alexa-568-labeled goat-anti-rabbit IgG was used and fluorescence signal intensity evaluated at 568 nm. Cell surface fluorescence signals for αvβ3 were recorded at 488 nm. The fluorescence images of ADAM15 and αvβ3 were merged in order to detect close neighbourhood of ADAM15 and αvβ3 expression in OV-MZ-6 cells.

OV-MZ-6 cell adhesion to VN by more than 90% but not to any of the other ECM proteins tested (Hapke et al., 2001). Based on these findings, we used OV-MZ-6 cells to study the impact of human ADAM15 on αvβ3-dependent cell adhesion. For this purpose, ADAM15 overexpressing as well as wild-type OV-MZ-6 cells displaying a moderate amount of ADAM15 were passed to cell culture dishes pretreated with VN, Col-IV, or Col-I. OV-MZ-6 cells expressing elevated levels of ADAM15 (FL-RGD) or its truncated version Ecto-RGD showed an up to three-fold reduced adhesive strength to VN ($p = 0.0495$), whereas identical OV-MZ-6 cell clones attached to Col-I-, Col-IV-, or non-coated cell culture dishes remained unchanged when compared to wild-type or vector-transfected cells. In contrast, OV-MZ-6 cell clones expressing either FL-SGA or Ecto-SGA did not display an altered adhesion profile to VN or any of the other ECM proteins tested (Table 1). Up to three alternative and independently isolated OV-MZ-6 cell clones of each transfection category with comparable ADAM15 expression levels were tested displaying similar adhesion profiles (data not shown). In order to validate the effects of ADAM15 on αvβ3-mediated OV-MZ-6 cell adhesion, we employed an alternative cell culture model by stably transfecting CHO cells with the four different ADAM15 cDNA constructs and performed in vitro cell adhesion tests. Likewise, CHO cells expressing either FL-RGD or Ecto-RGD exhibited a significantly decreased cell adhesive capacity exclusively towards VN, even not as pronounced as seen in OV-MZ-6 cells (∼2-fold reduction, $p = 0.0495$) (Table 1). Expression of ADAM15 FL-SGA or Ecto-SGA did not affect CHO cell adhesion to either ECM protein or to non-coated cell culture dishes when compared to wild-type or vector-transfected CHO cells (Table 1).

3.4. Elevation of ADAM15-RGD expression causes a time-dependent decline of numbers of OV-MZ-6 cells adherent to vitronectin

We next investigated the proliferative behavior of OV-MZ-6 cells as a function of ADAM15 expression levels. For this, we seeded OV-MZ-6 cells onto purified ECM proteins and determined cell numbers after distinct time intervals by counting. OV-MZ-6 cells expressing elevated levels of ADAM15 FL-RGD or Ecto-RGD and being adherent to VN exhibited a prominent

Table 1
Adhesion of ADAM 15 (over)expressing OV-MZ-6 clones to different purified ECM proteins

Cell type	OV-MZ-6				CHO			
	None[a]	VN[a]	Col-I[a]	Col-IV[a]	None[a]	VN[a]	Col-I[a]	Col-IV[a]
Wild-type	0.237 ± 0.007	0.598 ± 0.011	0.214 ± 0.01	0.436 ± 0.011	0.304 ± 0.026	0.563 ± 0.012	0.284 ± 0.004	0.529 ± 0.016
Vector	0.236 ± 0.008	0.583 ± 0.008 ($p = 0.2752$, n.s.)	0.296 ± 0.008	0.426 ± 0.016	0.298 ± 0.008	0.495 ± 0.014 ($p = 0.0495$)	0.253 ± 0.016	0.477 ± 0.012
FL-RGD	0.196 ± 0.008	0.231 ± 0.01 ($p = 0.0495$)	0.215 ± 0.013	0.478 ± 0.01	0.267 ± 0.008	0.273 ± 0.016 ($p = 0.0495$)	0.308 ± 0.019	0.489 ± 0.018
Ecto-RGD	0.235 ± 0.013	0.211 ± 0.01 ($p = 0.0495$)	0.276 ± 0.012	0.435 ± 0.011	0.209 ± 0.013	0.321 ± 0.017 ($p = 0.0495$)	0.309 ± 0.021	0.421 ± 0.017
FL-SGA	0.275 ± 0.009	0.591 ± 0.01 ($p > 0.999$, n.s.)	0.305 ± 0.011	0.391 ± 0.015	0.255 ± 0.017	0.487 ± 0.011 ($p = 0.0495$)	0.295 ± 0.023	0.559 ± 0.009
Ecto-SGA	0.272 ± 0.004	0.486 ± 0.01 ($p = 0.0495$	0.322 ± 0.017	0.419 ± 0.014	0.232 ± 0.013	0.527 ± 0.01 ($p = 0.0495$)	0.199 ± 0.026	0.575 ± 0.011

Adhesion assays were performed by chromogenic assays and subsequent spectrophoto-metrical measurements as described under Section 2 using either the ECM proteins VN, Col-I, or Col-IV as growth substrata as well as non-pretreated cell culture dishes as controls. Depicted are mean values (±S.D.) ($A_{405\,nm}$) of three independent determinations. Significance of differences in data were determined by one-tailed non-parametric Mann–Whitney tests (n.s. = not significant).

[a] ECM.

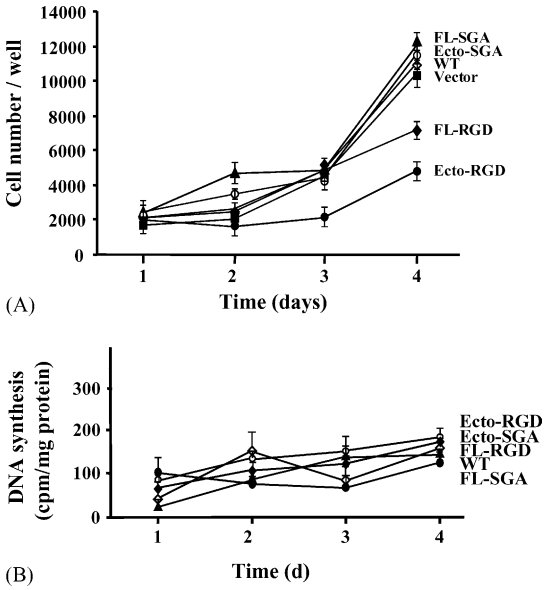

Fig. 3. Effect of ADAM15 expression on OV-MZ-6 cell proliferation. (A) Cell counts. Cell culture plates were coated with VN and 5×10^3 cells/96-well of each ADAM15-transfected OV-MZ-6 cell clone were plated and incubated for up to 4 days. After distinct time intervals, cells were washed in PBS and cell numbers determined. Depicted are mean values of three independent determinations. (B) [^{3}H]-methyl thymidine DNA incorporation test. ADAM15-expressing OV-MZ-6 cell clones were plated at a density of 2×10^4 cells per wells on VN-coated cell culture plates and incubated for up to 4 days. Every 24 h, [^{3}H]-methyl thymidine incorporation into cellular DNA was determined as described. cpm values were normalized to the protein concentration of each cell sample harvested in parallel. Depicted are mean values (±S.D.).

reduction in cell numbers within 4 days when compared to wild-type or vector-transfected OV-MZ-6 cells (Fig. 3A). Identical, transfected OV-MZ-6 cell clones attached to any of the other ECM proteins did not exert reduced cell numbers (data not shown). In contrast, adhesion of OV-MZ-6 cells expressing ADAM15 FL-SGA or Ecto-SGA to VN showed cell numbers comparable to wild-type and vector-transfected cells (Fig. 3A). In addition, cell growth as a function of ADAM15 expression was monitored by MTT proliferation assays confirming the data from the cell counting experiments (data not shown). Human ovarian OV-MZ-6 cancer cells are of epithelial origin and strictly anchorage-dependent, also with respect to cell growth. Thus, we next investigated whether the observed time-dependent decline in cell numbers as a function of ADAM15-RGD expression on VN was a direct consequence of diminished adhesive strength or due to altered cell proliferative activity by monitoring [^{3}H]-thymidine incorporation as a measure of de novo DNA synthesis. In all OV-MZ-6 cell transfectants tested, we did not observe any significant differences in the rate of DNA synthesis indicating that the observed differences in growth rates (see Fig. 3A) are due to loss of cells by detachment of ADAM15-RGD expressing OV-MZ-6 cells from VN (Fig. 3B).

3.5. ADAM15-RGD expression decreases integrin αvβ3-dependent random cell motility of OV-MZ-6 cells adherent to vitronectin

In in vitro cell migration assays, we studied whether ADAM15-dependent changes in cell-ECM adhesion might also affect the motile phenotype of human OV-MZ-6 cells. By conducting time lapse laser scanning microscopy, we measured track lengths of individual cells during 8 h of random cell migration (for an example of a motility experiment see Fig. 4A). At least 30 cells per experiment were evaluated exhibiting in all cases a Gausian distribution of track lengths (Fig. 4A). The migration assays were repeated at least three times for individual ADAM15-transfected OV-MZ-6 cell clones either attached to VN or Col-IV. The observed ADAM15-dependent modulation of αvβ3-mediated OV-MZ-6 cell adhesion to VN appeared to consequently also affect cellular motility. For OV-MZ-6 cells being attached to VN and exhibiting elevated ADAM15-RGD expression, we noticed a significant decrease in cellular motility. Cultivation of ADAM15-SGA-expressing cell clones on VN resulted in a similar migratory phenotype as observed for vector-transfected cells. ADAM15-transfected OV-MZ-6 cells of either category did not show significant changes of cell motility when cultivated on Col-IV (Fig. 4B).

4. Discussion

Integrin-mediated cell adhesion and continuous adaptation of the avidity of the interaction between cells and the surrounding ECM are essential for many (patho-)physiological processes, including tumor cell adhesion, migration, and proliferation (Felding-Habermann, 2003). In most ovarian cancer cells,

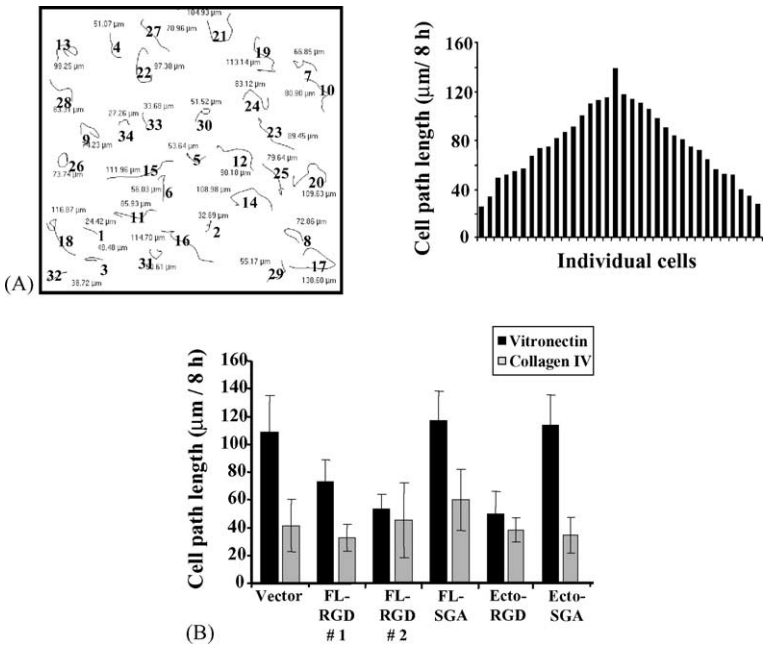

Fig. 4. OV-MZ-6 cell motility as a function of ADAM15 expression. Cell motility was recorded by time lapse laser scanning microscopy as described. Starting after 50 min, phase contrast images were taken every other 3 min within 8 h at 543 nm. Cell path lengths of cells based on the movement of the center of the nuclei were determined as described under Section 2. (A) Example of a motility experiment with OV-MZ-6 cells overexpressing ADAM15 FL-RGD seeded onto VN. Shown are cell tracks of 34 cells within 8 h. Respective Gausian distributions of cell path lengths was observed for all experiments evaluated. (B) Random cell motility as a function of ADAM15 expression. ADAM15-expressing OV-MZ-6 cell clones of each transfection category were seeded either on VN or Col-IV-coated cell culture dishes and random cellular motility followed over 8 h. Data are depicted as the mean of median values of cell track length (μm/8 h) (±S.D.) of at least 30 cells per experiment of each individual ADAM15-transfected OV-MZ-6 cell clone which was repeated at least three times on each ECM protein.

integrin αvβ3 is expressed and in parallel its ligand VN (Carreiras et al., 1999). Moreover, in primary ovarian cancer, αvβ3 is detected at a significantly higher rate than in ovarian tumors of low malignant potential, a fact which points to its role during ovarian cancer progression (Liapis, Adler, Wick, & Rader, 1997). In our previous work, we demonstrated that cell adhesion, proliferation, and migration of human ovarian OV-MZ-6 cancer cells in vitro can be significantly induced in an αvβ3/VN-dependent fashion (Hapke et al., 2003). In recent years, many experimental approaches have aimed at specifically interrupting αvβ3-mediated tumor cell adhesion to the underlying ECM by employing, e.g. specific antibodies directed to integrins, synthetic RGD-containing peptides, or peptidomimetics. Since in recent years, members of the growing ADAM protein family have been recognized as naturally occuring integrin interaction partners, their possible antagonistic role during integrin-dependent cellular adhesion and migration has also become an increasingly exciting cancer research topic. Indeed, some ADAMs have already been implicated in cancer (Black et al., 1997; Emi et al., 1993; O'Shea et al., 2000). ADAM15 due to its binding capacity towards αvβ3, thus also might be an important regulator of integrin-dependent tumorbiological functions. It should be emphasized here that human ADAM15 is the only ADAM which contains an RGD motif within its disintegrin region and its interaction with RGD-recognizing integrins has been somewhat anticipated. Most interestingly, the RGD motif of ADAM15 is not conserved among different species (mouse and rat ADAM15 contain the tripeptide motif Thr-Asp-Asp [TDD]) indicating that exclusively human ADAM15 can be considered a genuine αvβ3 ligand (Lum et al., 1998).

The capacity of ADAM15 to bind to αvβ3 has been reported by others from studies employing ADAM15-derived peptides, recombinant, soluble ADAM15 proteins, or hybrid molecules containing ADAM15 fragments (Eto et al., 2000; Nath et al., 1999, 2000; Zhang et al., 1998; Zhou et al., 2001). As such, Nath et al. (1999) performed cell adhesion assays with haematopoetic cells using an immobilized chimeric protein containing the extracellular portion of ADAM15 fused to the Fc region of human immunoglobulins and demonstrated that ADAM15 specifically binds to αvβ3 on monocytic U937 cells. Zhang et al. (1998) expressed a recombinant ADAM15 disintegrin-like domain fused to glutathione *S*-transferase (GST) in bacteria and also demonstrated that the ADAM15 disintegrin-like domain specifically interacts with αvβ3. Still, the experimental systems decribed above might not reflect the exact nature of the physiological functions of cell surface-expressed ADAM15 since the native conformation of recombinant fragments or peptides might not be preserved under these conditions, especially when they are immobilized on solid supports. Therefore, within the present study, we investigated αvβ3-binding functions of ADAM15 within a cellular context by generating human ovarian cancer cell transfectants displaying elevated amounts of ADAM15 and respective disintegrin domain mutants thereof. Since it has been hypothesized before by others that a fragment of ADAM15 containing the metalloprotease and disintegrin-like domain could be shed from cell surfaces (Herren et al., 1997), in addition, we transfected OV-MZ-6 cells with human ADAM15 cDNA constructs encompassing solely its extracellular portion in order to mimic a diffusible ADAM15-derived integrin ligand. In in vitro cell adhesion assays, we found that αvβ3-mediated interaction of human OV-MZ-6 and also CHO cells with VN was significantly impaired as a function of ADAM15 protein expression, an effect which was strictly RGD-dependent. Thereby, upon overexpression of ADAM15-RGD and a concomitant moderate expression of αvβ3, contact sites of the latter to the underlying ECM protein VN may become weakened. Indeed, by double immunostaining, we found a very similar distribution pattern of ADAM15 and αvβ3 on the OV-MZ-6 cell surface suggesting their possible interaction on the tumor cell surface.

Because cellular motility is also crucial for invasion of tumor cells into surrounding tissue and represents an adhesion-dependent, largely integrin-mediated biological event, we next studied whether the motile phenotype of OV-MZ-6 cells changes as a function of ADAM15 expression levels. We found that OV-MZ-6 cells decreased their motility on VN when overexpressing ADAM15 encompassing an intact RGD motif. This is in line with findings by Martin and co-workers (2002) who showed that human mesangial cell migration was blocked by antibodies directed to ADAM15 as well as by ADAM15 antisense oligodeoxynucleotides. In this study, treatment of cells with the metalloprotease inhibitor BB3103 also abrogated migration, suggesting that the metalloprotease activity is essential for this process. This is so far the only report pointing to an active metalloprotease function of ADAM15. In contrast, it was shown by others (Herren et al., 2001) that elevated ADAM15 inhibits NIH3T3 cell migration on fibronectin. This effect depended on increased cell/cell interactions and is consistent with the observation that ADAM15 localizes to cellular adherens junctions (Ham, Levkau, Raines, & Herren, 2002). However, no increased ADAM15-dependent cell–cell adhesion was observed in the human ovarian cancer cells used in the present study (data not shown).

Since proliferation is an adhesion-dependent phenomenon in anchorage-dependent tumor cells we studied whether the proliferative behavior of human OV-MZ-6 cells was changed as a function of increased ADAM15 synthesis. We noticed that ADAM15 expression reduced numbers of cells adherent to VN over time in an RGD-dependent fashion. The cell loss, however, was found to be rather a direct consequence of diminished αvβ3-dependent cell adhesive strength towards VN than caused by reduced cell proliferative activity.

The exact mechanisms, however, by which ADAM15 might interfere with integrin-mediated cell/ECM- and cell/cell-contacts as well as intracellular signaling events within a physiological context await further elucidation. Additional studies, including an analysis of ADAM15 expression in tumor tissue, will be necessary to further evaluate the potential use of ADAM15 as a target for cancer therapy.

References

Arndt, M., Lendeckel, U., Rocken, C., Nepple, K., Wolke, C., Spiess, A., et al. (2002). Altered expression of ADAMs (a disintegrin and

metalloproteinase) in fibrillating human atria. *Circulation*, *105*, 720–725.

Black, R. A., Rauch, C. T., Kozlosky, C. J., Peschon, J. J., Slack, J. L., Wolfson, M. F., et al. (1997). A metalloproteinase disintegrin that releases tumour necrosis factor-alpha from cells. *Nature*, *385*, 729–733.

Blobel, C. P. (1997). Metalloprotease-disintegrins: Links to cell adhesion and cleavage of TNF alpha and Notch. *Cell*, *90*, 589–592.

Böhm, B. B., Aigner, T., Blobel, C. P., Kalden, J. R., & Burkhardt, H. (2001). Highly enhanced expression of the disintegrin metalloproteinase MDC15 (metargidin) in rheumatoid synovial tissue. *Arthritis and Rheumatism*, *44*, 2046–2054.

Böhm, B. B., Aigner, T., Gehrsitz, A., Blobel, C. P., Kalden, J. R., & Burkhardt, H. (1999). Up-regulation of MDC15 (metargidin) messenger RNA in human osteoarthritic cartilage. *Arthritis and Rheumatism*, *42*, 1946–1950.

Bosse, F., Petzold, G., Greiner-Petter, R., Pippirs, U., Gillen, C., & Muller, H. W. (2000). Cellular localization of the disintegrin CRII-7/rMDC15 mRNA in rat PNS and CNS and regulated expression in postnatal development and after nerve injury. *Glia*, *32*, 313–327.

Bridges, L. C., Hanson, K. R., Tani, P. H., Mather, T., & Bowditch, R. D. (2003). Integrin α4β1-dependent adhesion to ADAM 28 (MDC-L) requires an extended surface of the disintegrin domain. *Biochemistry*, *42*, 3734–3741.

Brooks, P. C., Montgomery, A. M., Rosenfeld, M., Reisfeld, R. A., Hu, T., Klier, G., et al. (1994). Alpha v beta 3 antagonists promote tumor regression by inducing apoptosis of angiogenic blood vessels. *Cell*, *79*, 1157–1164.

Buxbaum, J. D., Liu, K. N., Luo, Y., Slack, J. L., Stocking, K. L., Peschon, J. J., et al. (1998). Evidence that tumor necrosis factor alpha converting enzyme is involved in regulated alpha-secretase cleavage of the Alzheimer amyloid precursor protein. *Journal of Biological Chemistry*, *273*, 27765–27767.

Carmichael, J., DeGraff, W. G., Gazdar, A. F., Minna, J. D., & Mitchell, J. B. (1987). Evaluation of a tetrazolium-based semiautomated colorimetric assay: Assessment of chemosensitivity testing. *Cancer Research*, *47*, 936–942.

Carreiras, F., Cruet, S., Staedel, C., Sichel, F., & Gauduchon, P. (1999). Human ovarian adenocarcinoma cells synthesize vitronectin and use it to organize their adhesion. *Gynecological Oncology*, *72*, 312–322.

Cruet, S., Salamanca, C., Mitchell, G. W. E., & Auersperg, N. (1999). αvβ3 and vitronectin expression by normal ovarian surface epithelial cells: Role in cell adhesion and cell proliferation. *Gynecological Oncology*, *75*, 254–260.

Damsky, C. H., & Werb, Z. (1992). Signal transduction by integrin receptors for extracellular matrix: Cooperative processing of extracellular information. *Current Opinion on Cell Biology*, *4*, 772–781.

Emi, M., Fujiwara, Y., Ohata, H., Tsuda, H., Hirohashi, S., Koike, M., et al. (1993). Allelic loss at chromosome band 8p21.3-p22 is associated with progression of hepatocellular carcinoma. *Genes Chromosomes Cancer*, *7*, 152–157.

Eto, K., Puzon-McLaughlin, W., Sheppard, D., Sehara-Fujisawa, A., Zhang, X. P., & Takada, Y. (2000). RGD-independent binding of integrin α9β1 to the ADAM-12 and -15 disintegrin domains mediates cell–cell interaction. *Journal of Biological Chemistry*, *275*, 34922–34930.

Felding-Habermann, B. (2003). Integrin adhesion receptors in tumor metastasis. *Clinical and Experimental Metastasis*, *20*, 203–213.

Giancotti, F. G., & Ruoslahti, E. (1999). Integrin signaling. *Science*, *285*, 1028–1032.

Ham, C., Levkau, B., Raines, E. W., & Herren, B. (2002). ADAM15 is an adherens junction molecule whose surface expression can be driven by VE-cadherin. *Experimental Cell Research*, *279*, 239–247.

Hapke, S., Kessler, H., Arroyo de Prada, N., Benge, A., Schmitt, M., Lengyel, E., et al. (2001). Integrin alpha(v)beta(3)/vitronectin interaction affects expression of the urokinase system in human ovarian cancer cells. *Journal of Biological Chemistry*, *276*, 26340–26348.

Hapke, S., Kessler, H., Luber, B., Benge, A., Hutzler, P., Höfler, H., et al. (2003). Ovarian cancer cell proliferation and motility is induced by engagement of integrin αvβ3/vitronectin interaction. *Biological Chemistry*, *384*, 1073–1083.

Herren, B. (2002). ADAM-mediated shedding and adhesion: A vascular perspective. *News Physiological Sciences*, *17*, 73–76.

Herren, B., Garton, K. J., Coats, S., Bowen-Pope, D. F., Ross, R., & Raines, E. W. (2001). ADAM15 overexpression in NIH3T3 cells enhances cell–cell interactions. *Experimental Cell Research*, *271*, 152–160.

Herren, B., Raines, E., & Ross, R. (1997). Expression of a disintegrin-like protein in cultured human vascular cells in vivo. *FASEB J.*, *11*, 173–180.

Hynes, R. O., & Lander, A. D. (1992). Contact and adhesive specificities in the associations, migrations, and targeting of cells and axons. *Cell*, *68*, 303–322.

Kärkkäinen, I., Karhu, R., & Huovila, A. P. J. (2000). Assignment of the ADAM 15 gene to human chromosome band 1q21.3 by in situ hybridization. *Cytogenetics and Cell Genetics*, *88*, 206–207.

Kheradmand, F., & Werb, Z. (2002). Shedding light on sheddases: Role in growth and development. *Bioessays*, *24*, 8–12.

Krätzschmar, J., Lum, L., & Blobel, C. P. (1996). Metargidin, a membrane-anchored metalloprotease-disintegrin protein with an RGD integrin binding sequence. *Journal of Biological Chemistry*, *271*, 4593–4596.

Lammich, S., Kojro, E., Postina, R., Gilbert, S., Pfeiffer, R., Jasionowski, M., et al. (1996). Constitutive and regulated alpha-secretase cleavage of Alzheimer's amyloid precursor protein by a disintegrin metalloprotease. *Proceedings of the National Academy of Sciences of the United States of America*, *96*, 3922–3927.

Landegren, U. J. (1984). Measurement of cell numbers by means of the endogenous enzyme hexosaminidase: Applications to detection of lymphokines and cell surface antigens. *Immunological Methods*, *67*, 379–388.

Liapis, H., Adler, L. M., Wick, M. R., & Rader, J. S. (1997). Expression of αvβ3 integrin is less frequent in ovarian epithelial tumors of low malignant potential in contrast to ovarian carcinomas. *Human Pathology*, *28*, 443–449.

Lum, L., Reid, M. S., & Blobel, C. P. (1998). Intracellular maturation of the mouse metalloprotease disintegrin MDC15. *Journal of Biological Chemistry*, *273*, 26236–26247.

Martin, J., Eynstone, L. V., Davies, M., Williams, J. D., & Steadman, R. (2002). The role of ADAM 15 in glomerular mesangial cell migration. *Journal of Biological Chemistry*, *277*, 33683–33689.

Möbus, V., Gerharz, C. D., Press, U., Moll, R., Beck, T., Mellin, W., et al. (1992). Morphological, immunohistochemical and biochemical characterization of 6 newly established human ovarian carcinoma cell lines. *International Journal of Cancer*, *52*, 76–84.

Nath, D., Slocombe, P. M., Stephens, P. E., Warn, A., Hutchinson, G. R., Yamada, K. M., et al. (1999). Interaction of metargidin (ADAM-15) with alphavbeta3 and alpha5beta1 integrins on different haemopoietic cells. *Journal of Cell Science*, *112*, 579–587.

Nath, D., Slocombe, P. M., Webster, A., Stephens, P. E., Docherty, A. J., & Murphy, G. (2000). Meltrin-γ (ADAM-9) mediates cellular adhesion through α6β1 integrin, leading to a marked induction of fibroblast cell motility. *Journal of Cell Science*, *113*, 2319–2328.

O'Shea, C., McKie, N., Buggy, Y., Duggan, C., Hill, A. D., McDermott, E., et al. (2003). Expression of ADAM-9 mRNA and protein in human breast cancer. *International Journal of Cancer*, *105*, 754–761.

Pan, D., & Rubin, G. M. (1997). Kuzbanian controls proteolytic processing of Notch and mediates lateral inhibition during Drosophila and vertebrate neurogenesis. *Cell*, *90*, 271–280.

Primakoff, P., & Myles, D. G. (2000). The ADAM gene family: Surface proteins with adhesion and protease activity. *Trends Genetics*, *16*, 83–87.

Qi, H., Rand, M. D., Wu, X., Sestan, N., Wang, W., Rakic, P., et al. (1999). Processing of the notch ligand delta by the metalloprotease Kuzbanian. *Science*, *283*, 91–94.

Reuning, U., Guerrini, L., Nishiguchi, T., Page, S., Seibold, H., Magdolen, V., et al. (1999). Rel transcription factors contribute to elevated urokinase expression in human ovarian carcinoma cells. *European Journal of Biochemistry*, *259*, 143–148.

Reuning, U., Wilhelm, O., Nishiguchi, T., Blasi, F., Graeff, H., & Schmitt, M. (1995). Inhibition of NF-kappa B-RelA expression by antisense oligodeoxynucleotides suppresses synthesis of urokinase-type plasminogen activator (uPA) but not its inhibitor PAI-1. *Nucleic Acids Research*, *23*, 3889–3893.

Ruoslahti, E., & Reed, J. C. (1994). Anchorage dependence, integrins, and apoptosis. *Cell*, *77*, 477–478.

Schwartz, M. A., & Ginsberg, M. H. (2001). Networks and crosstalk: Integrin signalling spreads. *Nature Cell Biology*, *4*, E65–E68.

Six, E., Ndiaye, D., Laabi, Y., Brou, C., Gupta-Rossi, N., Israel, A., et al. (2003). The Notch ligand delta1 is sequentially cleaved by an ADAM protease and gamma-secretase. *Proceedings of the National Academy of Sciences of the United States of America*, *100*, 7638–7643.

Van der Flier, A., & Sonnenberg, A. (2001). Function and interactions of integrins. *Cell and Tissue Research*, *305*, 285–298.

Weskamp, G., & Blobel, C. P. (1994). A family of cellular proteins related to snake venom disintegrins. *Proceedings of the National Academy of Sciences of the United States of America*, *91*, 748–751.

Wolfsberg, T. G., Primakoff, P., Myles, D. G., & White, J. M. (1995). ADAM, a novel family of membrane proteins containing a disintegrin and metalloprotease domain: Multipotential functions in cell–cell and cell–matrix interactions. *Journal of Cell Biology*, *131*, 275–278.

Wolfsberg, T. G., Straight, P. D., Gerena, R. L., Huovila, A. P., Primakoff, P., Myles, D. G., et al. (1995). ADAM, a widely distributed and developmentally regulated gene family encoding membrane proteins with a disintegrin and metalloprotease domain. *Developmental Biology*, *169*, 378–383.

Wolfsberg, T. G., & White, J. M. (1996). ADAMs in fertilization and development. *Developmental Biology*, *180*, 389–401.

Wu, E., Croucher, P. I., & McKie, N. (1997). Expression of members of the novel membrane linked metalloproteinase family ADAM in cells derived from a range of haematological malignancies. *Biochemical and Biophysical Research Communications*, *235*, 437–442.

Zhang, X. P., Kamata, T., Yokoyama, K., Puzon-McLaughlin, W., & Takada, Y. (1998). Specific interaction of the recombinant disintegrin-like domain of MDC-15 (metargidin, ADAM-15) with integrin alphav beta3. *Journal of Biological Chemistry*, *273*, 7345–7350.

Zhou, M., Graham, R., Russell, G., & Croucher, P. I. (2001). MDC-9 (ADAM-9/meltrin-γ) functions as an adhesion molecule by binding the αvβ5 integrin. *Biochemical Biophysical Research Communications*, *280*, 574–580.